Journal of New Materials for Electrochemical Systems 18, 095-102 (2015)

Prickly Nickel Nanowires Grown on Cu-Ni Substrate Surface as High Performance Cathodes for Hydrogen Evolution Reaction

Reza Karimi Shervedani, Akbar Amini and Motahareh Karevan

Department of Chemistry, University of Isfahan, Isfahan 81746-73441, I. R. IRAN

Received: September 4, 2014, Accepted: March 2, 2015, Available online: June 30, 2015

Abstract: *A new and highly rough nickel electrode is fabricated based on in-situ assembling of prickly nickel nanowires, synthesized by electroless deposition method on a layer of nickel freshly preelectrodeposited on copper, constructing Cu-Ni-PNNWs. Then, the fabricated electrode is studied for Hydrogen Evolution Reaction (HER). Surface morphology of the electrodes is characterized by Field Emission Scanning Electron Microscopy (FESEM) and X-ray diffraction (XRD) microanalysis. Kinetics of the HER is studied in 0.5 M H_2SO_4 on Cu-Ni-PNNWs electrode in comparison with Ni and Cu-Ni electrodes. Evaluation of the electrode activities is carried out by steady-state polarization curves (Tafel plots) and electrochemical impedance spectroscopy (EIS). The results obtained by electrochemical characterizations have shown that the Cu-Ni-PNNWs electrode benefits of high electrocatalytic activity for the HER. The EIS data are approximated using appropriate equivalent circuit model, and values of the model parameters are extracted. Analysis of the EIS results has revealed that the double layer capacitance (C_{dl}) and exchange current density (j_0) of the Cu-Ni-PNNWs electrode are increased by factors of ~ 47 and ~ 19 times, respectively, compared with Cu-Ni. Up to our knowledge, this is the first finding of this type, reporting synthesis and activity of the Cu-Ni-PNNWs electrode for the HER.*

Keywords: Prickly nickel nanowires; Hydrogen evolution reaction; Ni electroless deposition; Electrocatalysis

1. INTRODUCTION

Hydrogen is considered as an interesting energy carrier that can be an alternative to fossil fuels because of its numerous advantages, such as reusing, pollution-free and so on [1,2]. There are many techniques that produce hydrogen, among them, water electrolysis is an environmentally friendly method, and a highly promising technology to produce high purity hydrogen [3]. The water electrolysis involves an electrochemical reaction to decompose water under sufficient voltage drive. Unfortunately, the polarization loss due to HER is the major limiting factor in the energy-conversion efficiency of the cells.

To reduce over-potentials for the HER, a variety of electrocatalysts has been explored. The most active catalysts for HER are noble metals such as platinum or platinum-based alloys, due to their high electroactivity [4,5]. However, their large scale application is suffered from disadvantages of prohibitively high cost and low stability, which have been becoming major obstacles for the commercialization of the cells.

*To whom correspondence should be addressed:
Email: : rkarimi@sci.ui.ac.ir, rkarimi4531@yahoo.com
Phone: +98-31-37932715. Fax: +98-31-36689732

Therefore, to make water electrolysis more efficient and economical, selecting inexpensive electrode materials, which have high electrochemical activity, good time stability and low over-potential (η) for the HER at reasonably acceptable cathodic current density, are needed.

The most studied electrode material is nickel, its alloys and compounds. Nickel exhibits a high initial electrocatalytic activity toward the HER. However, it experiences extensive deactivation as a cathode during alkaline water electrolysis [6-12].

Enhancement of the cathodic activity of nickel for electrolytic hydrogen evolution has been carried out by (i) increasing intrinsic activity of electrode materials by use of multi-component catalysts (i.e. using synergistic effect) and/or (ii) increasing the active surface area (surface roughness) [11,13]. In addition, for long-term electrolysis, the electrode materials must resist against corrosion and retain their activity.

Various methods have been developed to increase the real surface area of Ni electrodes [14-16]; such as depositing Ni together with an active metal by electrodeposition [17,18] or forming a composite coating [19]. Herranz developed a 3D porous Ni electrode by electrodeposition of Ni on copper foams obtained from

hydrogen bubbles dynamic templates [20]. Prickly nickel nanowires (PNNWs) materials prepared by electroless deposition from aqueous solution phase have attracted considerable attentions recently, due to their prospects in fabricating devices for magnetic, electronic, and electrochemical sensor [21].

However, to our knowledge, there is no previous report regarding fabrication and kinetic studies of the PNNWs on the conductive electrode surface. An array of PNNWs on the electrode surface like Cu-Ni, if it is possible to be fabricated, can help one to benefit of PNNWs potential merits like high *stability* (metal-metal bond between Cu-Ni and *in-situ prepared* PNNWs) and *large surface area* of PNNWs together with their good *electrocatalytic activity* for different electrochemical applications, for example construction of the sensor and biosensor, and fabrication of the active cathodes for the HER.

A group of Raney-nickel materials had been synthesized and their activities were quantitatively studied for the HER in our previous works [11,22], where the most active electrode for the HER, Ni-Zn-P [22], was prepared via continuous layer-by-layer electrodeposition (three-step) method: (i) a layer of Ni from a Watts's bath, (ii) a layer of Ni-P on Ni by using bath (i) containing phosphorous acid, and (iii) the last layer, Ni-Zn-P from bath (ii) containing $ZnCl_2$. This type of fabrication, however, surfers at least from one important limitation: the electrodeposition bath solution is a one-time use solution. Thus, the method is expensive and cannot be commercialized. To overcome this drawback, one may use PNNWs to benefit of their large real surface and high stability. On the contrary to the previous works [11], the bath used for deposition of PNNNWs contains one type of metal ion reagent, Ni(II), accordingly, the concentration of the reagents can be controlled and adjusted, and thus, the bath can be reused.

Herein, we describe the synthesis and application of PNNWs, formed on the surface of Cu-Ni electrode base, toward the HER for the first time. The synthesis is performed by direct electroless assembling of PNNWs on a thin layer of Ni freshly and electrochemically predeposited on a copper electrode surface (Cu covered by a fresh layer of Ni) forming Cu-Ni-PNNWs electrode.

The surface morphology of the electrode is characterized by Field Emission Scanning Electron Microscopy (FESEM) and X-ray diffraction (XRD) microanalysis. The electrocatalytic performance of the developed electrode toward the HER is evaluated in an acidic solution by using steady-state polarization curves (Tafel plots) and electrochemical impedance spectroscopy (EIS) techniques.

2. EXPERIMENTAL

2.1. Material and Reagents

Nickel sulfate ($NiSO_4 \cdot 6H_2O$), nickel chloride ($NiCl_2 \cdot 6H_2O$), sodium hydroxide (NaOH), boric acid (H_3BO_3), Triton X-100 [$(C_{14}H_{22}O\ (C_2H_4O)_n)$], hydrazine hydrate ($N_2H_4\ H_2O$; 99%) and other chemicals were of analytical grade obtained from commercial sources (Sigma-Aldrich® or Merck®). All other reagents were of analytical grade. Double distilled water was used throughout the experiments.

2.2. Preparation of Cu-Ni-PNNWs electrode

Electrodeposition of Ni was carried out on a copper substrate having an exposed area of 0.237 cm^2. The copper substrate was made of a Cu rod (99.99%) sealed in a commercially available Teflon® rod exposing a two-dimensional surface area for the electrodeposition of Ni coating.

Before electrodeposition, the Cu substrate was polished with sandpaper (P 600, Siawat®), washed with water, immersed in a 1:1HNO_3:H_2O, washed with ethanol, and immediately introduced into the cell for electrodeposition. The *electrodeposition* of Ni was performed in a bath containing 1.14 M $NiSO_4$, 0.19 M $NiCl_2$, 0.49 M H_3BO_3 during 20 min, at 25 °C under galvanostatic condition 22 mA cm^{-2} [11,22]. The *freshly prepared Cu-Ni* was transferred to the *electroless* deposition bath to form the Cu-Ni-PNNWs electrode.

In a typical and selective synthesis of PNNWs with a sharp slender prickly surface, a precursor aqueous solution of $NiCl_2$ (10 mL; 0.05 M) was transferred into an aqueous solution of TX-100 (10 mL, 0.05 M) under continuous stirring conditions for 2 h, and the resulting green clear solution was transferred into a 100 mL flask along with the shaking, followed by slow heating at ~82ºC on a water bath. After *a while* (~30 min), 50 μL of 1.0 M NaOH solution was added with a subsequent addition of 1.0 mL of 99% $N_2H_4\ H_2O$ (we could not get acceptable results in the condition given by literature [23], thus, the aforementioned conditions are a modified version of this method). Finally, the *freshly prepared Cu-Ni* electrode was immersed into the flask where PNNWs were forming, and followed by shaking (not magnetic stirring!) the solution for 40 min [23]. After a while, the PNNWs were start forming on the Cu-Ni electrode by means of *electroless deposition* (Cu-Ni-PNNWs). The process was completed after a period of about 40 min (optimized). The modified electrode was removed and washed several times with water to drain out any physical adsorbed species (the excess of surfactant or hydrazine), and finally, washed with ethanol and used for characterization.

2.3. Apparatus and physicochemical characterization

Scanning electron microscopic (SEM) images were acquired using a Field Emission Scanning Electron Microscope (FESEM, Hitachi S4160, Cold Field Emission, JAPAN). XRD analysis of the samples was performed on a Bruker D8 Advance powder diffractometer using Ni filtered Cu-Kα radiation.

All the electrochemical studies were performed at 25 ±2 °C in a three-electrode glass cell including a Ag/AgCl (3 M KCl) electrode as the reference, a Pt plate as the counter electrode, and the PNNWs electrode as the working electrode. All the potentials are measured and reported vs. Ag/AgCl (3 M KCl). The CV and EIS measurements were carried out on Potentiostat/Galvanostat Autolab 302N equipped with a frequency response analyzer, and controlled by Nova 1.8 software (Eco Chemie, Utrecht, the Netherlands; N.B.). The electrolyte was 0.5 M H_2SO_4 aqueous solution saturated with argon gas for 30 min prior to the electrochemical test.

For details of data acquisition, modeling, and analysis of the results obtained for kinetic parameters, one may consult with the previous works (for example please see references [11,22]).

3. RESULTS AND DISCUSSION

3.1. Synthesis and characterization of Cu-Ni-PNNWs electrode

The formation process of PNNWs has been illustrated mechanis-

Scheme 1. Representation of laboratory set for fabrication of Cu-Ni-PNNWs electrode.

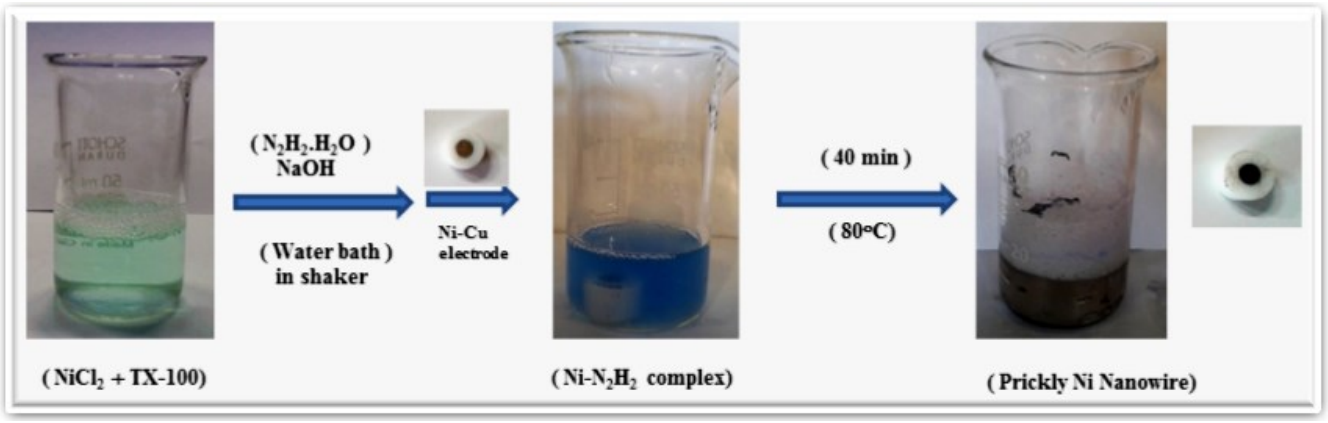

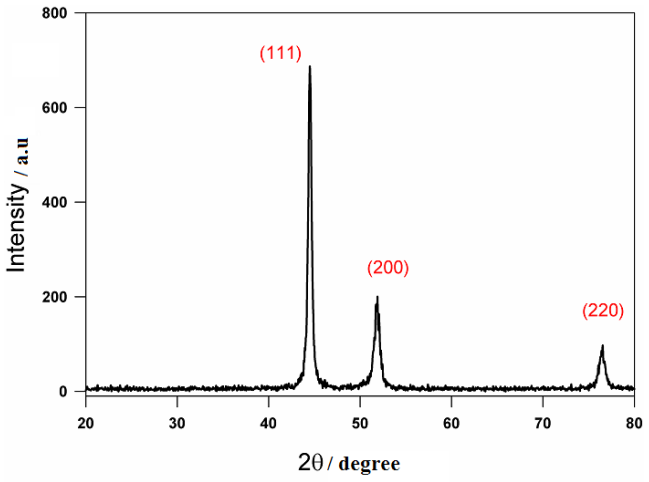

Figure 1. XRD patterns obtained of PNNWs surface.

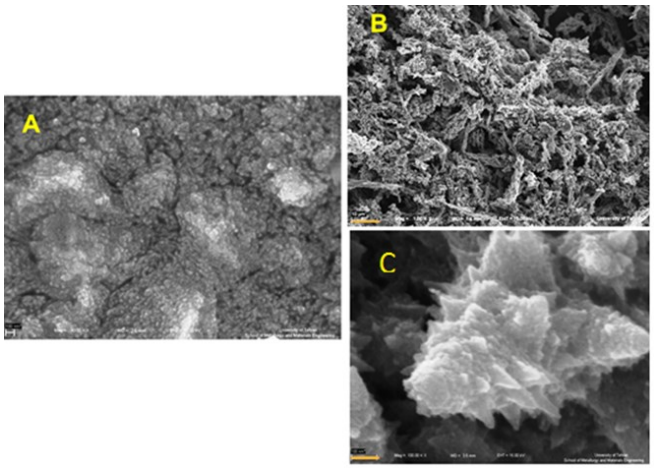

Figure 2. Panoramic FESEM images of (A) Cu-Ni (B) Cu-Ni-PNNWs. Preparation bath conditions: 0.05 M $NiCl_2$, $[Ni^{2+}]/[N_2H_4]$ = 0.026, 0.025 M T X-100 and shaking of the reaction solution mixture). See the text, Section 2.2 for details.

tically in Scheme 1. In the present research, PNNWs are grown on Cu-Ni substrates by *in-situ* method, using a simple, cost effective and reproducible electroless strategy. To the best of our knowledge, this is the first fabrication of PNNWs on the solid conductive surface using the extremely facile approach.

The successful fabrication of PNNWs was confirmed by powder XRD. A typical XRD pattern of the as-synthesized samples (Fig. 1) shows three characteristic diffraction peaks positioned at 44.4°, 51.6°, and76.5° that should be attributed to the (111), (200), and (220) crystalline planes of the face-centered cubic (Fcc) Ni. These statistics are in good agreement with the data reported for synthesized nickel nanowires. In addition, the broadening of the peaks in the pattern indicates the nanoscale dimensionality of the crystallites [23].

The FESEM images of the PNNWs formed on Cu-Ni substrate are depicted in Fig. 2. The image of the relatively smooth superficial Ni layer, prepared by *electrodeposition* of Ni on Cu base, is depicted in Fig. 2A. It is clear that the superficial morphology of the developed PNNWs catalyst, prepared by *electroless* deposition of Ni on Cu-Ni (Fig. 2B), is different from that of Cu-Ni (Fig. 2A). In addition, a high-magnification FESEM image, displaying a clear and separate nanowire with distinct spiky texture formed on the top of Cu-Ni surface, is presented in Fig. 2C. These vertically grown nano-dimensional branches are standing along the radial directions from the nanowires backbone at electrode surface.

3.2. Kinetics of the hydrogen evolution reaction

Kinetics of the HER was studied in a 0.5 M H_2SO_4 solution on two electrodes; Cu-Ni and Cu-Ni-PNNWs by recording steady-state polarization curves. The corresponding data obtained at scan rate of 5 mVs^{-1} at room temperature are presented in Fig. 3A.

Two interesting points could be suggested and explained in this case: (i) the onset potential of the HER at Cu-Ni-PNNWs is about 220 mV more positive than that observed on Cu-Ni electrode. So it is obvious that the electrocatalytic activity of the Cu-Ni electrode towards HER has significantly improved after deposition of the PNNWs on the electrode surface. (ii) The Cu-Ni-PNNWs electrode has exhibited larger current responses. This behavior is most probably due to increase in the number of active sites on the electrode surface (according to the Fig. 2) for the HER. These attributes need

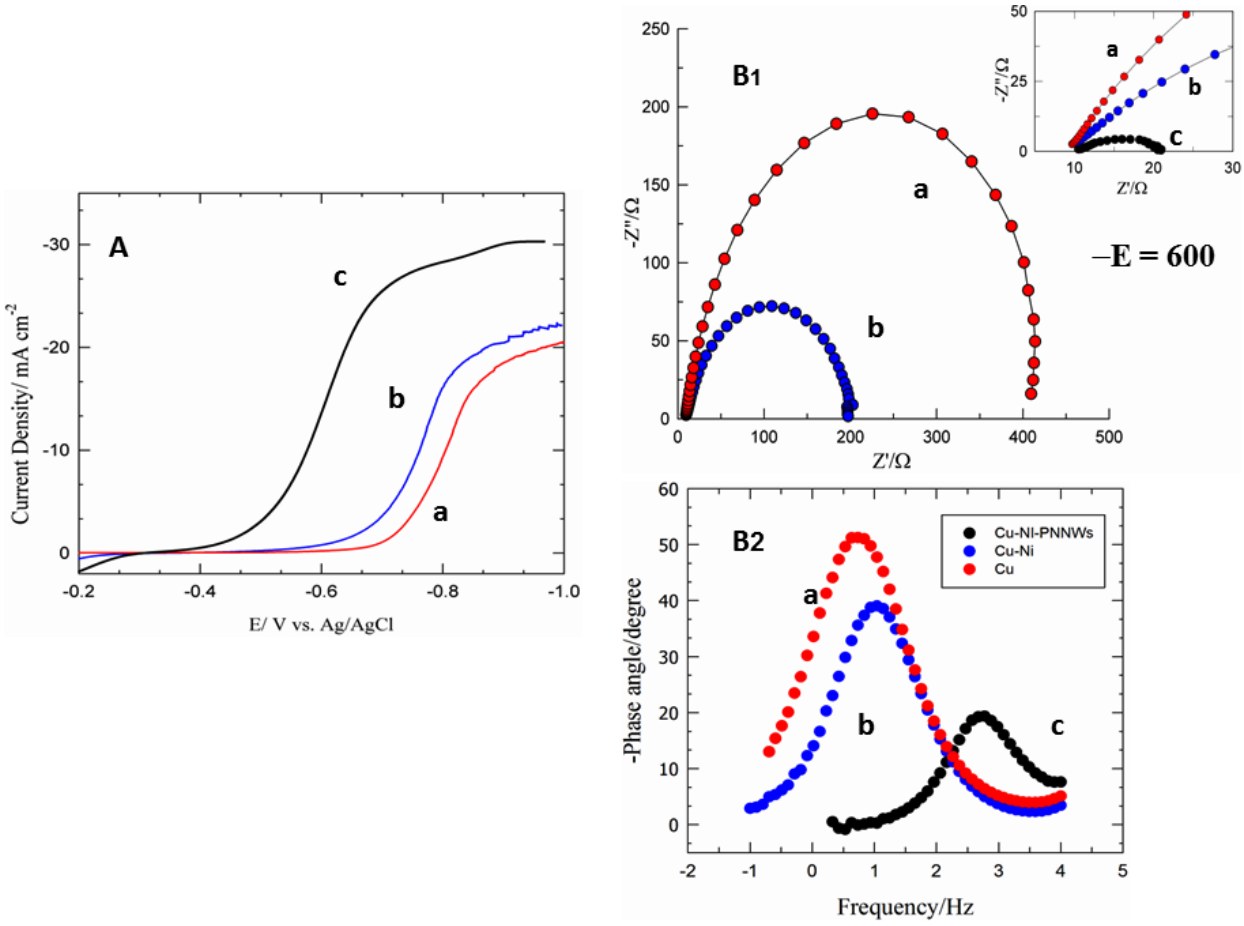

Figure 3. (A) Steady-state polarization curves of Cu (a), Cu-Ni (b), Cu-Ni-PNNWs electrode in 0.50 M H_2SO_4 solution at 25ºC. (B1) The EIS complex plane (Nyquist) plots and (B2) the phase angle (Bode) plots obtained for a 5 mV AC potential in the frequency range of 10 kHz to 100 mHz, superimposed on a constant DC potential (EDC = −600 mV), in the same conditions as (A).

more improvements. The results obtained by careful analysis of Tafel plots (Section 3.2.1) and the EIS data (Section 3.2.2) support the above mentioned attributes.

3.2.1. Steady state polarization curves (Tafel plots)

It is well established that the mechanisms of the HER in acidic solutions proceeds through the following steps [24]:

$$H_3O^+ + e + M \leftrightarrow M\text{-}H_{ads} + H_2O \quad (1)$$

$$M\text{-}H_{ads} + H_3O^+ + e \leftrightarrow H_2 + H_2O + M \quad (2)$$

$$M\text{-}H_{ads} + M\text{-}H_{ads} \leftrightarrow H_2 + H_2O \quad (3)$$

Where M represents the electrode materials and $M\text{-}H_{ads}$ the hydrogen adsorbed on the electrode surface.

Kinetic parameters, including exchange current density (j_0) and Tafel slopes (b) are obtained for the HER on Cu-Ni-PNNWs in comparison with Cu-Ni by fitting the linear part of the Tafel plots (Fig. 4) into the Tafel equation, E= -b log(j_0) + b log(j), based on linear least square (LLS) approximation method [11,22], where E is experimental measured potential, E^0 is equilibrium potential for the HER, b is Tafel slope, and j_0 is exchange current density, are presented in Table 1. The values of j_0, which provides information about the electrocatalytic activity of the electrode [25] clearly exhibited that the Cu-Ni-PNNWs electrode is characterized by higher apparent activity for the HER relative to Cu-Ni electrode. The j_0 of the Cu-Ni-PNNWs electrode was ~ 19 times larger than that of Cu-Ni electrode, which means that the exposed surface area is significantly increased upon this modification.

The Tafel slopes of Cu-Ni and Cu-Ni-PNNWs electrodes (-

Table 1. Kinetic parameters obtained from steady-states Tafel curves and the EIS for the HER in 0.5 M H_2SO_4.

	Tafel			EIS	
Electrode	b (mV dec^{-1})	j_0 (A cm^{-2})	α	b (mV dec^{-1})	j_0 (A cm^{-2})
Cu-Ni	157	3.15×10^{-6}	0.4	172	2.21×10^{-6}
PNNWs Ni-Cu	129	5.81×10^{-5}	0.51	143	3.91×10^{-5}

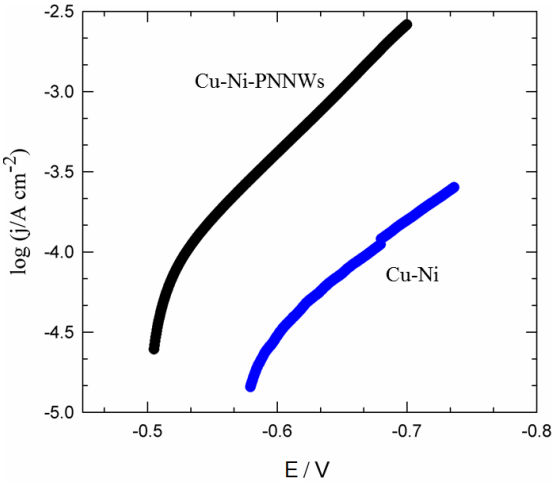

Figure 4. Steady-state polarization curves (Tafel plots) obtained in 0.50 M H_2SO_4 on investigated Cu, Cu-Ni and Cu-Ni-PNNWs electrodes. Symbols indicate experimental results and solid lines approximated data obtained using linear least squares (LLS) approximation.

157.0 mV dec^{-1} and -129 mV dec^{-1}, respectively) indicate that the HER on these electrodes has proceeded via a Volmer-Heyrovsky mechanism [26,27].

3.2.2. Electrochemical impedance spectroscopy (EIS)

The EIS is a powerful, nondestructive, amenable, and informative technique [28-30], which is usually used for characterization and study of the fuel cells and batteries [31,32], sensors and biosensors [33,34], active thin films [35] and biomolecules [36], and kinetics of the HER [37,38]. A brief, but interesting, review on the EIS is reported by Macdonald [39].

Typical models for the HER on solid electrodes contain a constant phase element (CPE) instead of the double layer capacitance [31,32]. Presence of the CPE was initially attributed to roughness or porosity (geometric factors) [40] and by the recent studies to the molecular and atomic scale inhomogeneities on the surface. Inhomogeneities arisen by adsorption of molecules and atoms or any defect cause a roughness at the atomic or molecular scale, can result in a deformation in the perfect semicircle circle [41,42], usually observed for a redox reaction on an ideal smooth electrode like Hg.

The EIS measurements obtained on the studied electrodes in this work including copper (Cu), electrodeposited of nickel on copper (Cu-Ni), and electroless deposited of PNNWs on Cu-Ni (i.e. Cu-Ni-PNNWs) displayed only one depressed semicircle on the complex plane plots at the entire range of the studied potentials. Examples of the EIS complex plane (B1) and Bode (B2) plots obtained on Cu-Ni and PNNWs electrode for a 5 mV AC potential in the frequency range of 10 kHz to 100 mHz, superimposed on a constant DC potential (E_{DC} = 600 mV) at 25 ^oC in 0.50 M H_2SO_4 solution are presented in Fig. 3 B1 & B2), indicating that that the charge-transfer resistance has decreased by step-by-step modification of the electrode surface from Cu base to Cu-Ni-PNNWs.

After testing the models related to the HER [11,31,32,43], considering the fit criteria such as ''number of model parameters'' and ''Chi square values''[11], the CPE model was found to be enough for approximations of the EIS data of the investigated electrodes. This model consists of a solution resistance (R_s) in series with the parallel connection of the CPE element and charge transfer resistance (R_{ct}). The faradaic impedance (Z_f) corresponding to one semicircle on the complex plane (Nyquist) plot is simply equal to R_{ct} [44,45]. The impedance of CPE is given as: $Z_{CPE} = 1/[T(j\omega)^{\varphi}]$, where T is a capacitive parameter related to the average double layer capacitance (C_{dl}) of the electrode [45,46]: $T = C_{dl}^{\varphi}[1/Rs + Rct]^{1-\varphi}j = (-1)^{1/2}$, ω is angular frequency, and φ is dispersion parameter which is related to the CPE model (the value of φ changes between zero to one, and is equal to one for complete smooth electrode, i.e. for φ= 1, $T = C_{dl}$).

To study more precisely the electrode activities, the EIS measurements were performed at the same conditions mentioned in Fig. 3B, but at *various DC potentials*. Examples of complex plane (A) and Bode (B) plots obtained on Cu-Ni-PNNWs electrode, in comparison with those obtained for Cu-Ni electrode, are presented in Figs. 5A1 & A2 and 5B1 & B2. The EIS data were approximated using ZViews® software and the modified complex nonlinear least square (CNLS) method [28,47]. The simulated curves are also presented in Fig. 5 as solid lines. Similar patterns are observed for the Cu electrode (See Supporting information, Fig. S1).

The kinetic parameters such as R_s, R_{ct}, C_{dl} and φ, obtained by fitting of the EIS data of Cu-Ni and Cu-Ni-PNNWs electrode are presented in Table 2. The R_{ct} values for Cu-Ni-PNNWs electrode are decreased by increasing potential, and are smaller at all studies potential in comparison with those of Cu-Ni electrode. A comparison between R_{ct} values from Cu-Ni to Cu-Ni-PNNWs indicates a significant decrease in R_{ct}, i.e. improvement in the electrocatalytic behavior of the Cu-Ni electrode for the HER upon modification with PNNWs.

The values of the parameter φ are close to unity and almost invariant in the range of the applied DC potential (See Supporting information, Fig S2). The closeness of φ to unity (e.g. 0.78 at the potential -600 mV) indicate that the surface inhomogeneities of the prickly nickel nanowires are in a few atomic scale [40-42], but larger than that of smooth Cu-Ni (where φ is ~0.78 at the potential -600 mV), which is normal. The constancy of the φ values implies that the homogeneities of the electrodes have not changed in the range of the applied DC potentials.

In addition, the results show that the C_{dl} has increased by a factor of ~47, from Cu-Ni to Cu-Ni-PNNWs electrode. Since electrochemically accessible active surface area is proportional to C_{dl}, it is evident that the number of active sites per unit of surface area of Cu-Ni-PNNWs electrode has been increased largely in comparison with that of Cu-Ni electrode.

The variations of C_{dl} as a function of the applied potential for the investigated electrodes (See Supporting information, Fig. S3) show a slow increase of C_{dl} by increasing the applied potential, indicating that the formation of gaseous hydrogen on the Cu-Ni-PNNWs surface does not decrease the real surface area [48]. The surface roughness factor, R_f, was calculated from the ratio of C_{dl} values of the tested electrodes to that of the smooth polycrystalline Ni electrode [49]: $R_f = C_{dl}/20$ mF cm^{-2}. The kinetic parameters of electrodes like φ, C_{dl} and R_f, obtained by EIS for the typical electrodes

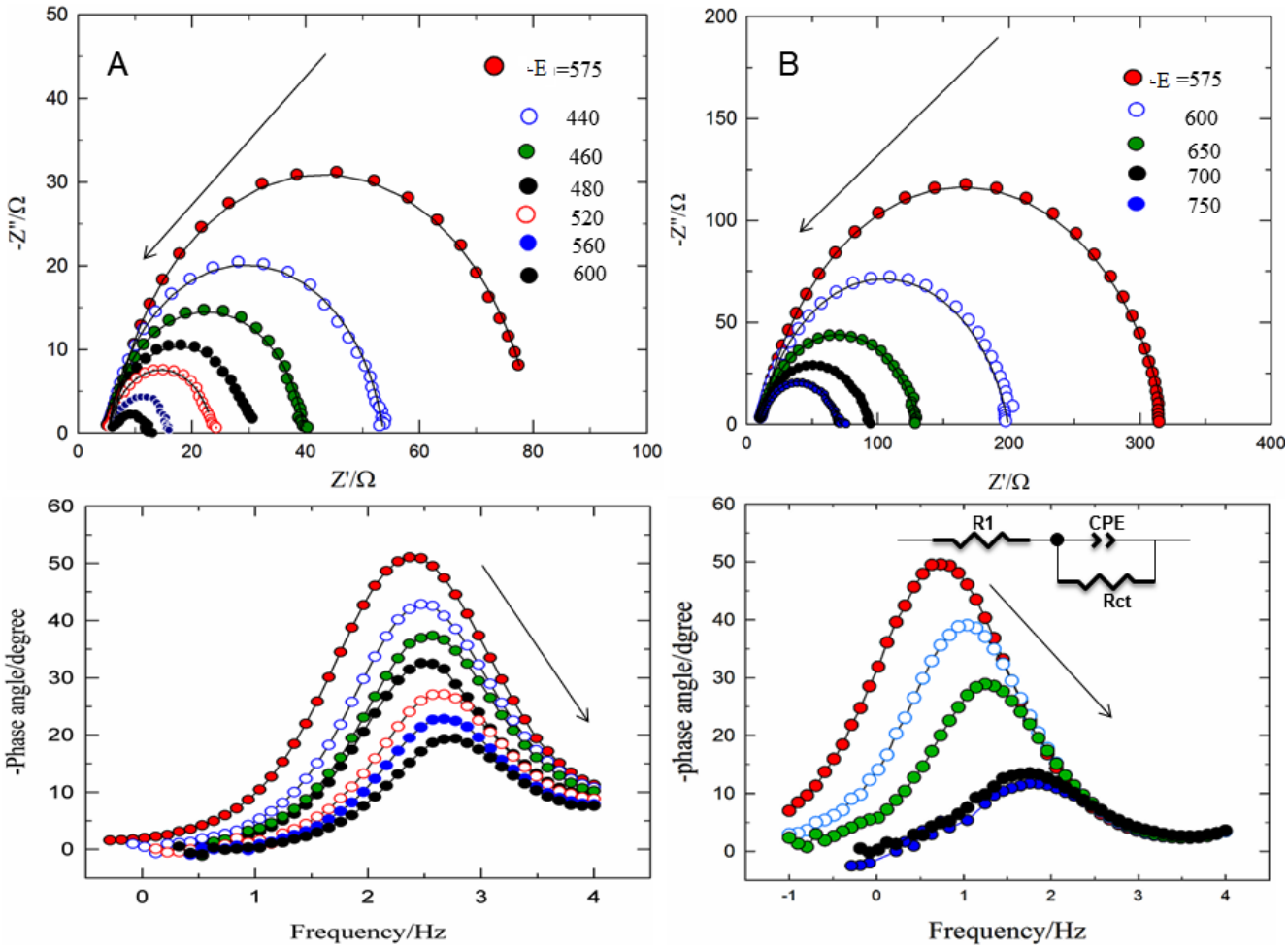

Figure 5. Complex plane and Bode plots of the EIS measurements obtained for the HER on (A) Cu-Ni-PNNWs and (B) Cu-Ni electrodes at various potentials in 0.50 M H_2SO_4. Symbols indicate experimental results and solid lines the data obtained by nonlinear least square approximation (NLSA) method based on one-CPE model.

Table 2. Kinetics parameters extracted from the EIS complex plane plots (Figure 4) obtained on Cu-Ni and Cu-Ni-PNNWs electrodes for HER in 0.5 M H_2SO_4.

		EIS			
electrode	-E	R_s/Ω	R_{ct}/Ω	C_{dl}/Fcm^{-2}	φ
	420	6.1 ± 0.1	73.78 ± 0.34	0.008	0.78
Cu-Ni	575	14.7 ± 0.6	309.3 ± 1.6	0.0016	0.83
	600	13.4 ± 1.7	191.2 ± 1.3	0.0017	0.83
	625	14.8 ± 0.9	135.7 ± 2.1	0.0018	0.85
	650	14.4 ± 0.3	92.3 ± 1.4	0.0025	0.84
	700	12.2 ± 0.2	75.5 ± 0.5	0.0031	0.82
Cu-Ni-PNNWs	440	5.9 ± 0.2	45.17 ± 0.27	0.0089	0.81
	460	5.2 ± 0.1	31.62 ± 0.22	0.0097	0.80
	480	5.7 ± 0.3	23.17 ± 0.37	0.01	0.79
	520	5.2 ± 0.2	16.31 ± 0.28	0.012	0.81
	560	5.7 ± 0.2	9.28 ± 0.19	0.013	0.81
	600	5.1 ± 0.1	5.73 ± 0.22	0.013	0.78

A simple model (Figure 5, inset Model M2), including a constant phase element (CPE) for double layer capacitance (C_{dl}) in series with solution resistant (R_s), was enough to explain the EIS data of Cu-Ni and Cu-Ni-PNNWs electrodes. The impedance of CPE is given as $Z_{CPE} = (Q(j\omega)^g)^{-1}$, $Q = C_{dl}{}^g [R_s{}^{-1} + R_{ct}{}^{-1}]^{1-g}$, where Q is related to the capacitance parameter, R_s and R_{ct} are solution and charge transfer resistances, $j = (-1)^{1/2}$, $\omega = 2\pi f$, f = frequency of the AC potential. The "g" parameter is dimensionless related to the rotation of the complex plane plot, which in turn is connected to the electrode surface inhomogeneity, so that for ideal smooth electrodes g = 1. The $Q = C_{dl}$ for smooth electrodes. The analysis of the EIS data was performed, according to the above assumptions, by using ZView2 (Scribner Associates, Inc.) based on the Macdonald's algorithm (LEVM7) using a complex non-linear least square (CNLS) approximation method. See Section 3.2.2 for details and fundamentals references.

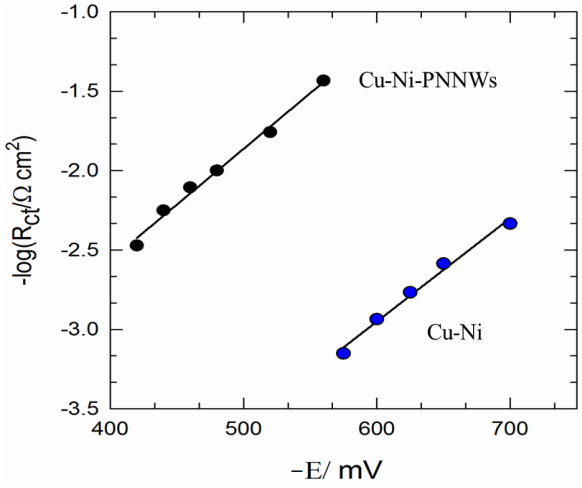

Figure 6. Dependence of inverse of the charge transfer resistance ($1/R_{ct}$) on E obtained for the HER in 0.5 M H_2SO_4 extracted from Figure 5. Symbols indicate experimental results and solid lines approximated data obtained by NLSA method.

are compared (Table 3), implying interesting behavior for Cu-Ni-PNNWs electrode.

Fig. 6 shows variations of the logarithm of the inverse charge transfer resistance ($1/R_c$) as a function of the potential. The linear relation observed between $\log(R_c^{-1})$ vs. E allowed us to determine a value for j_0 from the intercept by extrapolation of potential to zero value, which is reported to be a representative of the magnitude of the rate of the HER [50]. The value of the j_0 obtained from the EIS measurements are reasonably in agreement with the corresponding ones obtained from the Tafel plots (Table 1). The Tafel slopes, b, obtained for Cu-Ni and Cu-Ni-PNNWs electrodes by the EIS are slightly higher than those obtained from the Tafel plots. This difference could be influenced by experimental conditions.

The cathodic response of the Cu-NI-PNNWs toward the HER reached to a steady-state after a few minute HER in 0.5 M H_2SO_4 solution, and remained almost invariant after 17 days HER, as tested in this work. The electrode was removed, washed with water carefully, and kept in clean place when it was not in use. It showed excellent repeatability under these conditions.

From the results presented in this work, one can find a significant improvement in the kinetic parameter of the HER on Cu-Ni-PNNWs in comparison with Cu-Ni. This improvement is attributed to improvement of the real surface area via the new PNNWs nanostructure formed on the surface.

Table 3. Double layer capacitance and roughness factor obtained for the HER in 0.5 M H_2SO_4.

Electrode	EIS		
	φ[a]	$C_{dl,ave}$[b]/mF cm^{-2}	R_f[c]
Ni	…	0.02	1.0
Cu-Ni	0.82-0.85	0.23	11.5
Cu-Ni-PNNWs	0.78-0.81	10.8	540

[a]φ is dispersion parameter which is related to CPE model (see the text for details).
[b]Average double layer capacitance.
[c]Roughness factor assuming a double layer capacitance of 20 μFcm^{-2} for smooth polycrystalline nickel electrode.

4. CONCLUSION

Here, we have successfully developed a novel and high performance electrocatalyst based on PNNWs for the HER in acidic solutions. The fabrication process was easy and straightforward based on using aqueous solution baths in a two steps protocol; electrodeposition of a Ni prelayer on Cu substrate followed by electroless deposition strategy of PNNWs. The results obtained by steady-state polarization curves (Tafel plots) and the EIS measurements exhibited that the presence of the PNNWs coating can enhance surface area and the exchange current density of the HER by factors of 47 and 19, respectively, compared with the Cu-Ni. Finally, we believe that the proposed fabrication method could be extended to fabricate other metal or metal oxide modified electrodes for applications in a variety of fields, including sensor fabrication and the HER.

5. ACKNOWLEDGMENT

The authors gratefully acknowledge the University of Isfahan for financial supports and research facilities. Technical assistance from the University of Isfahan, Central Laboratory (UI-CL) is also acknowledged.

REFERENCES

[1] B.C.H. Steele, A. Heinzel, Nature, 414, 345 (2001).
[2] T. Hijikata, Int. J. Hydrogen Energy, 27, 115 (2002).
[3] A.J. Bard, M.A. Fox, Acc. Chem. Res., 28, 141 (1995).
[4] I.E.I. Stephens, I. Chorkendorff, Ange. Chem. Int. Ed., 50, 1476 (2011).
[5] M.J. Liao, Z.D. Wei, S.G. Chen, L. Li, M.B. Ji, Y.Q. Wang, Int. J. Hydrogen Energy, 35, 8071 (2010).
[6] M.A. Lukowski, A.S. Daniel, F. Meng, A. Forticaux, L. Li, S. Jin, J. Am. Chem. Soc., 135, 10274 (2013).
[7] H. Zheng, M. Mathe, Int. J. Hydrogen Energy, 36, 1960 (2011).
[8] N.V. Krstajic, V.D. Jovic, L.G. Krstajic, B.M. Jovic, A.L. Antozzi, G.N. Martelli, Int. J. Hydrogen Energy, 33, 3676 (2008).
[9] C. Hitz, A. Lasia, J. Electroanal. Chem., 500, 213 (2001).
[10] M. Xia, T. Lei, L. Ninglei, N. Li, Int. J. Hydrogen Energy, 39, 4794 (2014).
[11] R.K. Shervedani, A.R. Madram, Electrochim. Acta, 53, 426 (2007).
[12] R. Solmaz, A. Doner, G. Kardas, Electrochem. Commun., 10, 1909 (2008).
[13] I. Herraiz-Cardona, E. Ortega, J. García Antón, V. Pérez-Herranz, Int. J. Hydrogen. Energy, 36, 9428 (2011).
[14] D.F. Liang, J.J. Mallett, G. Zangari, J. Electrochem. Soc., 158, 149 (2011).
[15] R. Solmaz, A. Doumlner, G. Kardascedil, Int. J. Hydrogen Energy, 35, 10045 (2010).
[16] R. Solmaz, G. Kardas, Int. J. Hydrogen Energy, 135, 12079 (2011).
[17] I. Herraiz-Cardona, E. Ortega, V. Perez-Herranz, Electrochim. Acta, 56, 1308 (2011).
[18] G. Sheela, M. Pushpavanam, S. Pushpavanam, Int. J. Hydrogen Energy, 27, 627 (2002).
[19] Y. Choquette, L. Brossard, A. Lasia, Electrochim. Acta, 35,

1251 (1990).
[20]I. Herraiz-Cardona, E. Ortega, I. Vazquez-Gomez, V. Perez-Herranz, Int. J. Hydrogen Energy, 37, 2147 (2012).
[21]M. Mohl, A. Kumar, A.L.M. Reddy, A. Kukovecz, Z. Konya, I. Kiricsi, R. Vajtai, P.M. Ajaya, J, Phys. Chem., C 114, 389 (2010).
[22]R.K. Shervedani, A. Lasia, J. Electrochem. Soc., 144, 2652 (1997).
[23]T. Pals. Sarkar, A.K. Sinha, M. Pradhan, M. Basu, Y. Negishi, J. Phys. Chem., C 115, 1659 (2011).
[24]O. Azizi, M. Jafarian, F. Gobal, H. Heli, M.G. Mahjani, Int. J. Hydrogen Energy, 32, 1755 (2007).
[25]B.E. Conway, B.V. Tilak, Electrochim. Acta, 47, 3571 (2002).
[26]Z. Xie, P. He, L. Du, F. Dong, K. Dai, T. Zhang, Electrochim. Acta, 88, 390 (2013).
[27]A. Lasia, Curr. Top. Electrochem., 2, 239 (1993).
[28]E. Barsoukov, J.R. Macdonald, Impedance spectroscopy, theory, experiment and applications, 2nd ed., New York, Wiley, 2005.
[29]R.K. Shervedani, S. Pourbeyram, Biosens. Bioelectron., 24, 2199 (2009).
[30]R.K. Shervedani, M. Bagherzadeh, Electrochim. Acta, 53, 6293 (2008).
[31]A. Lasia In: Conway B.E., White R.E. (Eds), Modern aspects of electrochemistry, New York, Kluwer Academic, Plenum Publishers, 35, 1 (2002).
[32]A. Lasia In: W. Vielstich, A. Lamm, H.A. Gasteiger (Eds), Handbook of fuel cells; fundamentals, technology and applications, Part 4, Hydrogen evolution reaction, Chichester, Wiley, 2, 416 (2003).
[33]R.K. Shervedani, Z. Akrami, H. Sabzyan, J. Phys. Chem., C 115, 8042 (2011).
[34]R.K. Shervedani, A. Amini, Electrochim. Acta, 121, 376 (2014).
[35]T.M. Nahir, E.F. Bowden, Electrochim Acta, 39, 2347 (1994).
[36]R.K. Shervedani, A. Amini, Bioelectrochemistry, 84, 25 (2012).
[37]C. Hitz, A. Lasia, J. Electroanal. Chem., 532, 133 (2002).
[38]F. Rosalbino, G. Scavino, M.A. Grande, J. Electroanal. Chem., 694, 114 (2013).
[39]D.D. Macdonald, Electrochim. Acta, 51, 1376 (2006).
[40]T. Pajkossy, J. Electroanal. Chem., 111, 111 (1994).
[41]Z. Kerner, T. Pajkossy, Electrochim. Acta, 46, 207 (2000).
[42]M.H. Martin, A. Lasia, Electrochim. Acta, 56, 8058 (2011).
[43]J. Kubisztal, A. Budniok, A. Lasia, Int. J. Hydrogen Energy, 32, 1211 (2007).
[44]D.A. Harrington, B.E. Conway, J. Electroanal. Chem., 221, 1 (1987).
[45]R.K. Shervedani, A.R. Madram, Int. J. Hydrogn Energy, 33, 2468 (2008).
[46]P. Elumalai, H.N. Vasan, N. Mumichandraiah, S.A. Shivashankar, J. Appl. Electrochem., 32, 1005 (2002).
[47]J.R. Macdonald, J. Schoonman, A.P. Lehner, J. Electroanal. Chem., 131, 77 (1982).
[48]J. Divisek, J. Electroanal. Chem., 214, 615 (1986).
[49]R.K. Shervedani, A. Lasia, J. Electrochem. Soc., 144, 511 (1997).
[50]I. Herraiz-Cardona, E. Ortega, J. GarcíaAntón, V. Pérez-Herranz, Int. J. Hydrogen Energy, 36, 9428 (2011).